International Journal of Information Technology, Vol. 14 No. 2, 2008

A Lyapunov-based Path Planning and Obstacle Avoidance for a Two-link Manipulator on a Wheeled Platform

Bibhya Sharma, Jito Vanualailai and Avinesh Prasad

School of Computing, Information & Mathematical Sciences
University of the South Pacific, Suva, FIJI
Email: sharma_b@usp.ac.fj, vanualailai@usp.ac.fj, prasad_ai@usp.ac.fj

Abstract

In this paper, we, show, for the first time, how the Direct Method of Lyapunov could be used to construct a Lyapunov function that controls the motion of a mobile manipulator system by guiding it to its goal whilst avoiding obstacles in *a priori* known workspace. The mobile manipulator, modelled via its kinematic constraints, consists of a coupling of a holonomic manipulator with a nonholonomic mobile base. It is guided to its target by *an attraction function* that is part of the Lyapunov function. It avoids fixed and artificial obstacles, which are created from the singularities and the kinematic and dynamic constraints in the system, via *obstacle avoidance functions* that also make up the Lyapunov function. Computer simulations are used to illustrate the effectiveness of the proposed Lyapunov-based method.

Keywords: Nonholonomic vehicles, Direct Method of Lyapunov, kinodynamic constraints, mobile manipulator.

Subject Classification 34A30; 49J15; 70E60; 93D15.

1 Introduction

Mobile manipulators systems are manipulators mounted on wheeled platforms – a coupling of holonomic manipulators with nonholonomic bases. The sustained high level of interest

over the last two decades in the motion control, obstacle avoidance control and coordination control of mobile manipulator systems is a reflection of the importance of such systems in many engineering projects including explorations, surveillance, mining and construction.

The work of Seraji in the early 1990s culminates in a 1998 publication [19], which is now considered a landmark in the literature of motion control of mobile manipulators comprising an arm mounted on a mobile base. By combining the nonholonomic base constraints, the desired end-effector motion, and the user-specified redundancy resolution goals, Seraji obtained a set of augmented differential kinematic equations, which he then solved to obtain the required rover and manipulator motions. In the same and succeeding years, several researchers proposed other novel techniques for the control of both holonomic and nonholonomic mobile robots. The work of following researchers are noteworthy: in 1998 by Perriera et al. [17], Huang et al. [9] and Foulon et al. [5],[6]; in 1999 by Foulon et al. [7]; in 2000 by Papadopoulos and Poulakakis [15]; in 2002 by Sugar and Kumar [23]; in 2003, Matsikis et al. [12], and in 2005, Xu et al. [28].

The presence of fixed and moving obstacles adds another difficult dimension to the motion control problem of mobile manipulators. Yamamoto and Yun, also in the early 1990s, tackled the problem of coordinating manipulators in the presence of obstacles, and solved it using an artificial potential fields approach [29]. In 2002, Papadopoulos et al. [14] formulated a solution to the obstacle avoidance problem of mobile manipulators using a polynomial-based approach, which they further improved in 2005 [13]. Another noteworthy contribution in this area is that of the work of Tanner et al. [24], who in 2003 introduced the concept of Dipolar Inverse Lyapunov Functions (DILFs) as sources of artificial potential fields for obstacle avoidance and the coordination of manipulators. Indeed, the work of Tanner et al. [24] firmly establishes the role of the Direct Method of Lyapunov as that of an artificial potential fields methodology that offers the greatest ease and flexibility in the synthesis of control laws for mobile manipulators. He showed that Lyapunov method could be easily used to construct DILFs from which discontinuous kinematic feedback control laws could be establish to guarantee global asymptotic stability for close loop mobile manipulator systems. In 2006 and 2007, Sharma et al. [21], [22] and Sharma [20], also used the Lyapunov method to construct Lyapunov functions that treat singularities and constraints in nonholonomic systems as artificial obstacles. It is appropriate to mention here that the concept of artificial potential fields itself was developed in the late 1980s and early 1990s, as can be seen in the pioneering work of Khatib [10] in 1986, Connolly et al. [3] in 1990, and Tarassenko and Blake [25], Kim and Khosla [11] in 1991, and Rimon and Koditschek [18] in 1992.

In this paper, the path planning and obstacle avoidance schemes developed earlier in Vanualailai et al.[26], [27] for manipulators with a fixed base are extended to the mobile manipulators. In doing so, we show, for the first time, how the Direct Method of Lyapunov could be used to construct a Lyapunov function that controls the motion of a mobile manipulator system by guiding it to its goal whilst treating constraints and singularities as artificial

obstacles that, together with real fixed obstacles, need to be avoided in *a priori* known workspace. The main advantage of this Lyapunov-based approach is the ease in which it can be used to solve the path-find problem and take into account system constraints. Moreover, it is easily applied to robotic systems.

The rest of the paper is organized as follows. In Section 2, the kinematic model of a planar mobile manipulator consisting of a car-like mobile platform and a mounted 2-link robotic arm. In Section 3, the control objective is described, and the targets and obstacles are defined. In Section 4, a Lyapunov function for the system is constructed and control laws are derived. Finally computer simulations are provided in Section 5.

2 Vehicle Model

The mobile manipulator consists of a rear wheel car-like (Reeds and Shepp's model) mobile platform with a 2-link planar arm mounted on the mid-front axle of the platform (see Fig. 1).

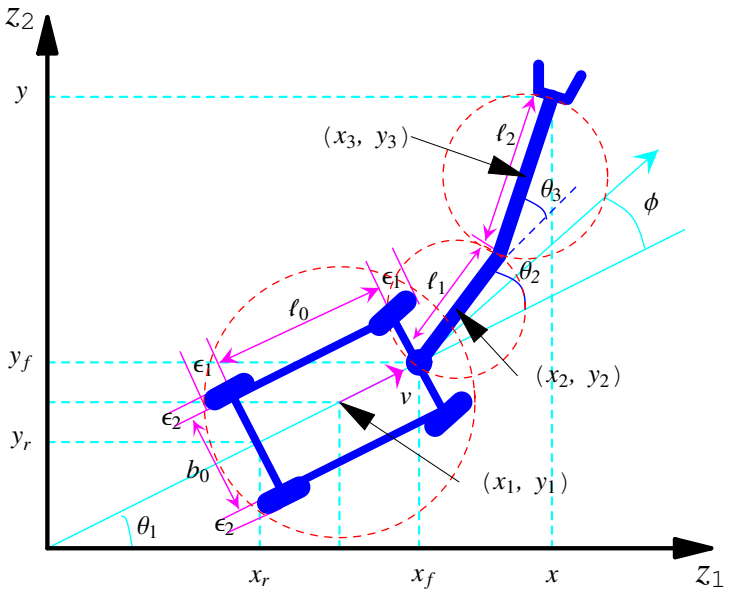

Fig. 1: Schematic representation of a 2-link mobile manipulator

With reference to Figure 1, point (x_1, y_1) locates the center of the platform, θ_1 is the orientation of the platform with respect to the z_1-axis, θ_2 is the orientation of the first link, Link 1, with respect to the platform, while θ_3 gives the orientation of the second link, Link 2, with respect to Link 1. Also ϕ gives the platforms steering angle with respect to

the its longitudinal axis, while ℓ_0 and b_0 are, respectively, the length and the width of the platform. Furthermore, ℓ_1 and ℓ_2 are the lengths of Link 1 and Link 2, respectively.

We shall now consider the governing equations of the mobile platform and the 2-link arm separately and then combine them effectively to obtain the governing ODEs of the entire mobile manipulator.

Firstly, from Pappas and Kyriakopoulos [16], we have that the kinematic model of the car-like platform with respect to its reference point (x_1, y_1) is

$$\begin{aligned}
\dot{x}_1 &= v\cos\theta_1 - \frac{\ell_0}{2}\omega_1\sin\theta_1, \\
\dot{y}_1 &= v\sin\theta_1 + \frac{\ell_0}{2}\omega_1\cos\theta_1, \\
\dot{\theta}_1 &= \omega_1, \qquad \dot{v} = u_1, \qquad \dot{\omega}_1 = u_2,
\end{aligned}$$

where v and ω_1 are its instantaneous translational and rotational velocities, respectively, and u_1 and u_2 are, the instantaneous translational and rotational accelerations, respectively.

Secondly, we consider the 2-link arm separately. Suppose that Link 1 is anchored at $(0, 0)$. Then the position (x_e, y_e) of the end-effector can be given by the kinematic equations

$$x_e = \ell_1\cos\theta_2 + \ell_2\cos(\theta_2+\theta_3)\ , \quad y_e = \ell_1\sin\theta_2 + \ell_2\sin(\theta_2+\theta_3).$$

Using these, we have the kinematic model of the 2-link arm as

$$\begin{aligned}
&\dot{x}_e = -\ell_1\omega_2\sin\theta_2 - \ell_2(\omega_2+\omega_3)\sin(\theta_2+\theta_3), \\
&\dot{y}_e = \ell_1\omega_2\cos\theta_2 + \ell_2(\omega_2+\omega_3)\cos(\theta_2+\theta_3), \\
&\dot{\theta}_2 = \omega_2, \quad \dot{\theta}_3 = \omega_3, \\
&\dot{\omega}_2 = u_3, \quad \dot{\omega}_3 = u_4,
\end{aligned}$$

where ω_2 and ω_3 are the instantaneous angular velocities, and u_3 and u_4 are the instantaneous angular accelerations, respectively, of Link 1 and Link 2.

Finally, we consider the car-like mobile platform and the 2-link arm together as a mobile manipulator, where the arm is mounted on the mid-front axle of the mobile platform. Accordingly, the position (x, y) of its end-effector, now relative to (x_1, y_1), can be rewritten as

$$\begin{aligned}
x &= x_1 + \frac{\ell_0}{2}\cos\theta_1 + \ell_1\cos(\theta_1+\theta_2) + \ell_2\cos(\theta_1+\theta_2+\theta_3), \\
y &= y_1 + \frac{\ell_0}{2}\sin\theta_1 + \ell_1\sin(\theta_1+\theta_2) + \ell_2\sin(\theta_1+\theta_2+\theta_3).
\end{aligned}$$

Then letting $\theta_T = (\theta_1+\theta_2+\theta_3)$ and $\omega_T = (\omega_1+\omega_2+\omega_3)$, it is straightforward to show

that a kinematic model of the mobile manipulator is

$$\left.\begin{array}{l} \dot{x} = v\cos\theta_1 - \ell_0\omega_1\sin\theta_1 - \ell_1(\omega_1+\omega_2)\sin(\theta_1+\theta_2) - \ell_2\omega_T\sin\theta_T, \\ \dot{y} = v\sin\theta_1 + \ell_0\omega_1\cos\theta_1 + \ell_1(\omega_1+\omega_2)\cos(\theta_1+\theta_2) + \ell_2\omega_T\cos\theta_T, \\ \dot{\theta}_1 = \omega_1, \qquad \dot{\theta}_2 = \omega_2, \qquad \dot{\theta}_3 = \omega_3, \\ \dot{v} = u_1, \qquad \dot{\omega}_1 = u_2, \qquad \dot{\omega}_2 = u_3, \qquad \dot{\omega}_3 = u_4. \end{array}\right\} \tag{1}$$

We shall use the vector notation $\mathbf{x} = (x, y, \theta_1, \theta_2, \theta_3, v, \omega_1, \omega_2, \omega_3) \in \mathbf{R}^9$ to refer to the position and the velocity components of the mobile manipulator. A system trajectory will be traced on the z_1z_2-plane by the point $(x, y) = (x(t), y(t))$ at every time $t \geq 0$.

We note that we can express the positions of the mobile platform, Link 1 and Link 2 completely in terms of the state variables x, y, θ_1, θ_2, and θ_3. For the mobile platform, we have

$$\left.\begin{array}{rcl} x_1 &=& x - \ell_2\cos(\theta_1+\theta_2+\theta_3) - \ell_1\cos(\theta_1+\theta_2) - \dfrac{\ell_0}{2}\cos\theta_1, \\ y_1 &=& y - \ell_2\sin(\theta_1+\theta_2+\theta_3) - \ell_1\sin(\theta_1+\theta_2) - \dfrac{\ell_0}{2}\sin\theta_1. \end{array}\right\} \tag{2}$$

For Link 1, we have

$$\left.\begin{array}{rcl} x_2 &=& x - \ell_2\cos(\theta_1+\theta_2+\theta_3) - \dfrac{\ell_1}{2}\cos(\theta_1+\theta_2), \\ y_2 &=& y - \ell_2\sin(\theta_1+\theta_2+\theta_3) - \dfrac{\ell_1}{2}\sin(\theta_1+\theta_2). \end{array}\right\} \tag{3}$$

For Link 2, we have

$$\left.\begin{array}{rcl} x_3 &=& x - \dfrac{\ell_2}{2}\cos(\theta_1+\theta_2+\theta_3), \\ y_3 &=& y - \dfrac{\ell_2}{2}\sin(\theta_1+\theta_2+\theta_3). \end{array}\right\} \tag{4}$$

These position constraints are known as the *holonomic constraints* of the mobile manipulator system.

3 Control Objective, Target and Obstacles

To ensure that the entire body of the mobile manipulator safely steers pass an obstacle, we enclose the planar robot by the smallest circle possible. Given the *clearance parameters* ϵ_1 and ϵ_2, we can enclose the platform by a circular protective region centered at (x_1, y_1) with radius $r_1 = \frac{1}{2}\sqrt{(\ell_0+2\epsilon_1)^2 + (b_0+2\epsilon_2)^2}$. For Link 1 and Link 2, we use circular protective regions centered at (x_2, y_2) and (x_3, y_3), with radius $r_2 = \ell_1/2$ and $r_3 = \ell_2/2 + \epsilon_3$ (where ϵ_3 is the clearance parameter needed to protect the gripper), respectively.

Our control objective is to control the motion of the mobile manipulator to its designated target while ensuring that it avoids all fixed obstacles within *a priori* known workspace.

Specifically, utilizing the Direct Method of Lyapunov, we want to design the acceleration controllers, u_1, u_2, u_3 and u_4 such that the mobile manipulator, represented by system (1), will navigate safely in a dynamic environment, reach a neighborhood of its target and be aligned to a pre-determined final posture. To obtain a feasible solution of this multi-task problem, we will use a Lyapunov function to generate artificial potential fields. The governing idea behind the an potential field approach, pioneered in 1986 by Khatib [10], is to attach attractive field to the target and a repulsive field to each of the obstacles. The whole workspace is then inundated with positive and negative fields, with the direction of motion facilitated via the notion of steepest descent.

We begin by describing precisely the target, the workspace, the parking bay, and all the obstacles that could potentially be encountered by the mobile manipulator.

3.1 Target

For the end-effector of the mobile manipulator, we have a designated target with center (a_1, a_2) and radius r_T and we define this target as

$$T = \left\{(z_1, z_2) \in \mathbb{R}^2 : (z_1 - a_1)^2 + (z_2 - a_2)^2 \leq r_T^2\right\}.$$

For attraction to this target, we define the function

$$V(\mathbf{x}) = \frac{1}{2}\left[(x - a_1)^2 + (y - a_2)^2 + v^2 + \omega_1^2 + \omega_2^2 + \omega_3^2\right],$$

which is a measure of the distance between the end-effector and its target, and the rate of approach of the end-effector to its target. If a_3, a_4 and a_5 are the final orientations of the platform, Link 1 and Link 2, respectively, when the end-effector is at the target T, then we can see that at $\mathbf{x} = \mathbf{x}_e := (a_1, a_2, a_3, a_4, a_5, 0, 0, 0, 0)$, we have $V = 0$. Hence if V is a part of a Lyapunov function for the system, then its role to ensure that system trajectories start and remain close to $\mathbf{x}_e$, so that $\mathbf{x}_e$ could be considered as a stable equilibrium point of system (1).

3.2 Fixed Obstacles from the Boundaries of the Workspace

Our workspace is a fixed, closed and bounded rectangular region, defined, for some $\eta_1 > 2(r_1 + r_2 + r_3)$ and $\eta_2 > 2(r_1 + r_2 + r_3)$, as

$$WS = \{(z_1, z_2) \in \mathbb{R}^2 : 0 \leq z_1 \leq \eta_1, 0 \leq z_2 \leq \eta_2\}.$$

We require the mobile manipulator to stay within the rectangular region at all time $t \geq 0$. The boundaries of the region are defined as follows:

(a) Left Boundary: $B_1 = \{(z_1, z_2) \in \mathbb{R}^2 : z_1 = 0\}$;

(b) Lower Boundary: $B_2 = \{(z_1, z_2) \in \mathbb{R}^2 : z_2 = 0\}$;

(c) Right Boundary: $B_3 = \{(z_1, z_2) \in \mathbb{R}^2 : z_1 = \eta_1\}$;

(d) Upper Boundary: $B_4 = \{(z_1, z_2) \in \mathbb{R}^2 : z_2 = \eta_2\}$.

These boundaries are considered as fixed obstacles, and they have to be avoided by the mobile manipulator. Now, since the two ends of Link 1 are protected by the protective circular regions of the mobile platform and of Link 2, respectively, it is sufficient to consider avoidance functions only for the mobile platform and Link 2. These functions are given in Table 1.

Table 1: Functions for the avoidance of the boundaries of the workspace.

Boundary	Avoidance by platform	Avoidance by Link 2
Left, B_1	$W_1(\mathbf{x}) = x_1 - r_1$	$W_5(\mathbf{x}) = x_3 - r_3$
Lower, B_2	$W_2(\mathbf{x}) = y_1 - r_1$	$W_6(\mathbf{x}) = y_3 - r_3$
Right, B_3	$W_3(\mathbf{x}) = \eta_1 - r_1 - x_1$	$W_7(\mathbf{x}) = \eta_1 - r_3 - x_3$
Upper, B_4	$W_4(\mathbf{x}) = \eta_2 - r_1 - y_1$	$W_8(\mathbf{x}) = \eta_2 - r_3 - y_3$

Now, since $\eta_1 > 2\,(r_1 + r_2 + r_3)$ and $\eta_2 > 2\,(r_1 + r_2 + r_3)$, each of the functions is positive in WS. That is, $W_1, W_3 > 0$ for all $x_1 \in (r_1, \eta_1 - r_1)$, $W_2, W_4 > 0$ for all $y_1 \in (r_1, \eta_2 - r_1)$, $W_5, W_7 > 0$ for all $x_3 \in (r_3, \eta_1 - r_3)$, and $W_6, W_8 > 0$ for all $y_3 \in (r_3, \eta_2 - r_3)$, recalling that the components of (x_1, y_1) and (x_3, y_3) are given in (2) and (4), respectively.

Following [20] and [21], each of these functions will be added as a ratio to a Lyapunov function of the system. Indeed, consider the effect of the ratios α_i/W_i for some constant $\alpha_i > 0$ and $i = 1, \ldots, 8$. When the mobile manipulator approaches a boundary of the workspace, one of the ratios will increase. Because the Lyapunov function is a nonincreasing function, this increase in the value of a ratio will result only in an increase in the absolute value of the time-derivative of the Lyapunov function. This, in turn, instigates an increase in the activity of the system. This increased activity could only be directed towards an equilibrium point of the system, away from the border. In other words, we cannot have a situation where $W_i = 0$, $i = 1, \ldots, 8$. Hence, if the ratios form parts of a Lyapunov function for system (1), intuitively the ratios will act as *obstacle avoidance functions*, which will restrict the articulated vehicle to operate within its rectangular workspace.

The essence of obstacle avoidance capability in our method lies, therefore, in the creation of obstacle avoidance functions that will induce an increase or decrease in the instantaneous rate of change of the Lyapunov function.

Henceforth, for each obstacle, we will construct an appropriate function that will appear in the denominator of an obstacle avoidance function.

3.3 Fixed Obstacles from the Boundaries of the Parking Bay

We consider a row-structured parking bay, with two parallel boundary lines, within which the mobile manipulator has to be parked. The two parallel boundary lines are obstacles to be avoided.

A boundary line is avoided by identifying and avoiding three points on the line: (i) that which is closest to the center of the mobile platform, (ii) that which is closest to the center of Link 1 and (iii) that which is closest to the center of Link 2. The avoidance of the closest point on the line at any time $t \geq 0$ essentially results in the avoidance of the entire line.

Specifically, consider the k^{th} line segment in the z_1z_2-plane with initial coordinates (a_{k1}, b_{k1}) and final coordinate (a_{k2}, b_{k2}). The parametric representation of the k^{th} line segment can be written as

$$c_{mk} = a_{k1} + \lambda_k(x_m, y_m)(a_{k2} - a_{k1}), \quad d_{mk} = b_{k1} + \lambda_k(x_m, y_m)(b_{k2} - b_{k1}).$$

Minimizing the Euclidian distance between the point (x_m, y_m) and the line segment (c_{mk}, d_{mk}), we get $\lambda_k(x_m, y_m) = (x_m - a_{k1})q_k + (y_m - b_{k1})r_k$, where

$$q_{k1} = \frac{(a_{k2} - a_{k1})}{(a_{k2} - a_{k1})^2 + (b_{k2} - b_{k1})^2}, \qquad q_{k2} = \frac{(b_{k2} - b_{k1})}{(a_{k2} - a_{k1})^2 + (b_{k2} - b_{k1})^2}.$$

where $\lambda_k(x_m, y_m) \in [0, 1]$. If $\lambda_k(x_m, y_m) \geq 1$, then we let $\lambda_k(x_m, y_m) = 1$, in which case $(c_{mk}, d_{mk}) = (a_{k2}, b_{k2})$ and if $\lambda_k(x_m, y_m) \leq 0$, then we let $\lambda_k(x_m, y_m) = 0$, in which case $(c_{mk}, d_{mk}) = (a_{k1}, b_{k1})$. Otherwise we accept the value of $\lambda_k(x_m, y_m)$ between 0 and 1.

To avoid the closest point on the k^{th} line of the parking bay, we shall use the function

$$LS_{mk}(\mathbf{x}) = \frac{1}{2}\left[(x_m - c_{mk})^2 + (y_m - d_{mk})^2 - r_m^2\right],$$

for $m = 1, 2, 3$, which represent the three points, and $k = 1, 2$, which represent the two parallel boundaries of the parking bay.

3.4 Other Fixed obstacles

Let us fix $q > 0$ obstacles within the boundaries of the workspace. We assume that the l^{th} obstacle is circular with center given as (p_{l1}, p_{l2}) and radius rad_l. We define the l^{th} obstacle as

$$O_l = \{(z_1, z_2) \in \mathbb{R}^2 : (z_1 - p_{l1})^2 + (z_2 - p_{l2})^2 \leq rad_l^2\},$$

for $l = 1, 2, \ldots, q$. For its avoidance we will need to have separate potential functions for platform and the two links. Thus we consider

$$FO_{ml}(\mathbf{x}) = \frac{1}{2}\left[(x_m - p_{l1})^2 + (y_m - p_{l2})^2 - (r_m + rad_l)^2\right],$$

for $m = 1, 2, 3$ and $l = 1, 2, \ldots, q$. The functions $FO_{1l}(\mathbf{x})$, $FO_{2l}(\mathbf{x})$ and $FO_{3l}(\mathbf{x})$ are measures of distances between the l^{th} obstacle and the platform, the l^{th} obstacle and Link 1, and the l^{th} obstacle and Link 2, respectively.

3.5 Artificial Obstacles from Dynamic Constraints

The instantaneous velocities of the mobile platforms and the links are restricted due to safety considerations, and the rotation angles of Link 1 and Link 2, are restricted due to mechanical singularities. Based on these dynamic constraints, we construct *artificial obstacles* to be avoided.

3.5.1 Modulus Bound on Velocities

Modulus bounds on the velocities are treated as dynamics constraints. If $v_{\max} > 0$ is the maximum speed of the mobile platform, and $\phi_{\max}$ is the maximum steering angle satisfying $0 < \phi_{\max} < \pi/2$, then, as shown in [16], the constraints imposed on the translational velocity, v, and the rotational velocity, ω, are

$$|v| \le v_{\max} \text{ and } v^2 \ge \rho_{\min}^2 \omega_1^2, \quad \rho_{\min} = L/\tan\phi_{\max}. \tag{5}$$

From (5), we easily have

$$|\omega_1| \le |v|/|\rho_{\min}| \le v_{\max}/|\rho_{\min}|. \tag{6}$$

For Link 1 and Link 2, we bound the instantaneous rotational velocities ω_2 and ω_3 by $\omega_{2\max}$ and $\omega_{3\max}$, respectively. That is, $|\omega_2| < \omega_{2\max}$ and $|\omega_3| < \omega_{3\max}$.

Based on each of these constraints, we construct the following artificial obstacles:

$$\begin{aligned}
AO_1 &= \{v \in \mathbb{R} : v \le -v_{\max} \text{ or } v \ge v_{\max}\};\\
AO_2 &= \{\omega_1 \in \mathbb{R} : \omega_1 \le -v_{\max}/|\rho_{\min}| \text{ or } \omega_1 \ge v_{\max}/|\rho_{\min}|\};\\
AO_3 &= \{\omega_2 \in \mathbb{R} : \omega_2 \le -\omega_{2\max} \text{ or } \omega_2 \ge \omega_{2\max}\};\\
AO_4 &= \{\omega_3 \in \mathbb{R} : \omega_3 \le -\omega_{3\max} \text{ or } \omega_3 \ge \omega_{3\max}\}.
\end{aligned}$$

For the avoidance of these artificial obstacles, we adopt the following functions, respectively,

$$\begin{aligned}
U_1(\mathbf{x}) &= \frac{1}{2}(v_{\max} - v)(v_{\max} + v),\\
U_2(\mathbf{x}) &= \frac{1}{2}\left(\frac{v_{\max}}{|\rho_{\min}|} - \omega_1\right)\left(\frac{v_{\max}}{|\rho_{\min}|} + \omega_1\right),\\
U_3(\mathbf{x}) &= \frac{1}{2}(\omega_{2\max} - \omega_2)(\omega_{2\max} + \omega_2),\\
U_4(\mathbf{x}) &= \frac{1}{2}(\omega_{3\max} - \omega_3)(\omega_{3\max} + \omega_3),
\end{aligned}$$

each of which will appear in the denominator of an obstacle avoidance function.

3.5.2 Mechanical singularities

A singular configuration arises when $\theta_3 = 0$, $\theta_3 = \pi$ or $\theta_3 = -\pi$. Consequently, the condition placed on θ_3 is $0 < |\theta_3| < \pi$, which means that the links can neither be fully stretched nor folded onto each other. For the avoidance of these singular configurations, we will use the following functions

$$S_1(\mathbf{x}) = |\theta_3| \quad \text{and} \quad S_2(\mathbf{x}) = \pi - |\theta_3|,$$

for $\theta_3 \in (-\pi, 0) \cup (0, \pi)$. Each function will be used to avoid the artificial obstacle defined as

$$AO_5 = \{\theta_3 \in \mathbb{R} : \theta_3 = 0, \theta_3 = \pi \text{ or } \theta_3 = -\pi\}.$$

We also note that the angle between Link 1 and the mobile platform is bounded, that is, $-\pi/2 < \theta_2 < \pi/2$. In other words, Link 1 can freely rotate within $(-\pi/2, \pi/2)$. To ensure that Link 1 stays within this interval, we will use

$$S_3(\mathbf{x}) = \frac{1}{2}\left(\frac{\pi}{2} - \theta_2\right)\left(\frac{\pi}{2} + \theta_2\right),$$

for the avoidance of the artificial obstacle defined as

$$AO_6 = \{\theta_2 \in \mathbb{R} : \theta_2 \leq -\frac{\pi}{2} \text{ or } \theta_2 \geq \frac{\pi}{2}\}.$$

3.6 Auxiliary Function

To ensure that our Lyapunov function vanishes at the target T defined earlier, we shall use the *auxiliary function*

$$F(\mathbf{x}) = \frac{1}{2}\left[(x-a_1)^2 + (y-a_2)^2 + \sum_{i=1}^{3}\zeta_i(\theta_i - a_{i+2})^2\right],$$

where a_3, a_4 and a_5 are the desired final orientations of the platform and the two links, noting that at the point $\mathbf{x} = \mathbf{x}_e = (a_1, a_2, a_3, a_4, a_5, 0, 0, 0, 0)$, we have $F = 0$. The constant ζ_i is a binary constant which we shall call the *angle-gain parameter* for $\theta_i, i = 1, 2, 3$. An angle-gain parameter will take a value of one only if a final pre-defined orientation is warranted, else it takes the default value of zero.

In the next section, we define a Lyapunov function for the system (1) such that the point $\mathbf{x}_e = (a_1, a_2, a_3, a_4, a_5, 0, 0, 0, 0)$ becomes a stable equilibrium point of the system.

4 Lyapunov Function

Introducing *control parameters* $\alpha_s > 0$, $\gamma_{ml} > 0$, $\psi_{mk} > 0$, $\xi_p > 0$, and $\beta_r > 0$, we define a Lyapunov function candidate for system (1) as

$$\begin{aligned} L(\mathbf{x}) \;=\; & V(\mathbf{x}) + F(\mathbf{x})\left[\sum_{s=1}^{8}\frac{\alpha_s}{W_s(\mathbf{x})} + \sum_{m=1}^{3}\left(\sum_{l=1}^{q}\frac{\gamma_{ml}}{FO_{ml}(\mathbf{x})} + \sum_{k=1}^{2}\frac{\psi_{mk}}{LS_{mk}(\mathbf{x})}\right)\right. \\ & \left. + \sum_{p=1}^{3}\frac{\xi_p}{S_p(\mathbf{x})} + \sum_{r=1}^{4}\frac{\beta_r}{U_r(\mathbf{x})}\right], \end{aligned} \tag{7}$$

which is defined, continuous and positive over the domain

$$\begin{aligned} D(L) \;=\; & \{\mathbf{x} \in \mathbb{R}^9 : W_s(\mathbf{x}) > 0, s = 1, \ldots, 8;\ S_p(\mathbf{x}) > 0, p = 1, 2, 3; \\ & FO_{ml}(\mathbf{x}) > 0, m = 1, 2, 3, l = 1, \ldots, q;\ U_r(\mathbf{x}) > 0, r = 1, \ldots, 4; \\ & LS_{mk}(\mathbf{x}) > 0, m = 1, 2, 3, k = 1, 2\}. \end{aligned}$$

We note that the point $\mathbf{x} = \mathbf{x}_e = (a_1, a_2, a_3, a_4, a_5, 0, 0, 0, 0)$ is in $D(L)$, and that $L(\mathbf{x}_e) = 0$.

4.1 Controller Design and Stability Analysis

Recalling that $\theta_T = \theta_1 + \theta_2 + \theta_3$, and defining $\theta_Q = \theta_1 + \theta_2$, the time-derivative of L along a trajectory of system system (1) is

$$\begin{aligned}
\dot{L}_{(1)}(\mathbf{x}) &= \left[(f_1 + f_3 + f_5 + f_7)\cos\theta_1 + (f_2 + f_4 + f_6 + f_8)\sin\theta_1 + h_1u_1\right]v \\
&\quad + \Bigg[-\left(f_1 + \frac{1}{2}f_3 + f_5 + f_7\right)\ell_0\sin\theta_1 + \left(f_2 + \frac{1}{2}f_4 + f_6 + f_8\right)\ell_0\cos\theta_1 \\
&\qquad - \left(f_1 + \frac{1}{2}f_5 + f_7\right)\ell_1\sin\theta_Q + \left(f_2 + \frac{1}{2}f_6 + f_8\right)\ell_1\cos\theta_Q \\
&\qquad - \left(f_1 + \frac{1}{2}f_7\right)\ell_2\sin\theta_T + \left(f_2 + \frac{1}{2}f_8\right)\ell_2\cos\theta_T + g_1 + h_2u_2\Bigg]\omega_1 \\
&\quad + \Bigg[-\left(f_1 + \frac{1}{2}f_5 + f_7\right)\ell_1\sin\theta_Q + \left(f_2 + \frac{1}{2}f_6 + f_8\right)\ell_1\cos\theta_Q \\
&\qquad - \left(f_1 + \frac{1}{2}f_7\right)\ell_2\sin\theta_T + \left(f_2 + \frac{1}{2}f_8\right)\ell_2\cos\theta_T + g_2 + h_3u_3\Bigg]\omega_2 \\
&\quad + \Bigg[-\left(f_1 + \frac{1}{2}f_7\right)\ell_2\sin\theta_T + \left(f_2 + \frac{1}{2}f_8\right)\ell_2\cos\theta_T + g_3 + h_4u_4\Bigg]\omega_3,
\end{aligned}$$

where the functions f_1 to f_8, g_1 to g_3 and h_1 to h_4 are defined below:

$$\begin{aligned}
f_1 &= \left[1 + \sum_{s=1}^{8}\frac{\alpha_s}{W_s} + \sum_{m=1}^{3}\left(\sum_{l=1}^{q}\frac{\gamma_{ml}}{FO_{ml}} + \sum_{k=1}^{2}\frac{\psi_{mk}}{LS_{mk}}\right) + \sum_{p=1}^{3}\frac{\xi_p}{S_p} + \sum_{r=1}^{4}\frac{\beta_r}{U_r}\right](x - a_1), \\
f_2 &= \left[1 + \sum_{s=1}^{8}\frac{\alpha_s}{W_s} + \sum_{m=1}^{3}\left(\sum_{l=1}^{q}\frac{\gamma_{ml}}{FO_{ml}} + \sum_{k=1}^{2}\frac{\psi_{mk}}{LS_{mk}}\right) + \sum_{p=1}^{3}\frac{\xi_p}{S_p} + \sum_{r=1}^{4}\frac{\beta_r}{U_r}\right](y - a_2), \\
f_3 &= \frac{\alpha_3 F}{W_3^2} - \frac{\alpha_1 F}{W_1^2} - \sum_{l=1}^{q}\frac{\gamma_{1l}F}{FO_{1l}^2}(x_1 - p_{l1}) \\
&\quad - \sum_{k=1}^{2}\frac{\psi_{1k}F}{LS_{1k}^2}\left[(1 - (a_{k2} - a_{k1})q_{k1})(x_1 - c_{1k}) - (b_{k2} - b_{k1})q_{k1}(y_1 - d_{1k})\right], \\
f_4 &= \frac{\alpha_4 F}{W_4^2} - \frac{\alpha_2 F}{W_2^2} - \sum_{l=1}^{q}\frac{\gamma_{1l}F}{FO_{1l}^2}(y_1 - p_{l2}) \\
&\quad - \sum_{k=1}^{2}\frac{\psi_{1k}F}{LS_{1k}^2}\left[(1 - (b_{k2} - b_{k1})q_{k2})(y_1 - d_{1k}) - (a_{k2} - a_{k1})q_{k2}(x_1 - c_{1k})\right],
\end{aligned}$$

$$
\begin{aligned}
f_5 &= -\sum_{l=1}^{q} \frac{\gamma_{2l} F}{FO_{2l}^2} (x_2 - p_{l1}) \\
&\quad -\sum_{k=1}^{2} \frac{\psi_{2k} F}{LS_{2k}^2} \left[(1 - (a_{k2} - a_{k1}) q_{k1}) (x_2 - c_{2k}) - (b_{k2} - b_{k1}) q_{k1} (y_2 - d_{2k}) \right], \\
f_6 &= -\sum_{l=1}^{q} \frac{\gamma_{2l} F}{FO_{2l}^2} (y_2 - p_{l2}) \\
&\quad -\sum_{k=1}^{2} \frac{\psi_{2k} F}{LS_{2k}^2} \left[(1 - (b_{k2} - b_{k1}) q_{k2}) (y_2 - d_{2k}) - (a_{k2} - a_{k1}) q_{k2} (x_2 - c_{2k}) \right], \\
f_7 &= \frac{\alpha_7 F}{W_7^2} - \frac{\alpha_5 F}{W_5^2} - \sum_{l=1}^{q} \frac{\gamma_{3l} F}{FO_{3l}^2} (x_3 - p_{l1}) \\
&\quad -\sum_{k=1}^{2} \frac{\psi_{3k} F}{LS_{3k}^2} \left[(1 - (a_{k2} - a_{k1}) q_{k1}) (x_3 - c_{3k}) - (b_{k2} - b_{k1}) q_{k1} (y_3 - d_{3k}) \right], \\
f_8 &= \frac{\alpha_8 F}{W_8^2} - \frac{\alpha_6 F}{W_6^2} - \sum_{l=1}^{q} \frac{\gamma_{3l} F}{FO_{3l}^2} (y_3 - p_{l2}) \\
&\quad -\sum_{k=1}^{2} \frac{\psi_{3k} F}{LS_{3k}^2} \left[(1 - (b_{k2} - b_{k1}) q_{k2}) (y_3 - d_{3k}) - (a_{k2} - a_{k1}) q_{k2} (x_3 - c_{3k}) \right], \\
g_1 &= \left[\sum_{s=1}^{8} \frac{\alpha_s}{W_s} + \sum_{m=1}^{3} \left(\sum_{l=1}^{q} \frac{\gamma_{ml}}{FO_{ml}} + \sum_{k=1}^{2} \frac{\psi_{mk}}{LS_{mk}} \right) + \sum_{p=1}^{3} \frac{\xi_p}{S_p} + \sum_{r=1}^{4} \frac{\beta_r}{U_r} \right] \zeta_1 (\theta_1 - a_3), \\
g_2 &= \left[\sum_{s=1}^{8} \frac{\alpha_s}{W_s} + \sum_{m=1}^{3} \left(\sum_{l=1}^{q} \frac{\gamma_{ml}}{FO_{ml}} + \sum_{k=1}^{2} \frac{\psi_{mk}}{LS_{mk}} \right) + \sum_{p=1}^{3} \frac{\xi_p}{S_p} + \sum_{r=1}^{4} \frac{\beta_r}{U_r} \right] \zeta_2 (\theta_2 - a_4) \\
&\quad + \frac{\xi_3 F}{S_3^2} \theta_2, \\
g_3 &= \left[\sum_{s=1}^{8} \frac{\alpha_s}{W_s} + \sum_{m=1}^{3} \left(\sum_{l=1}^{q} \frac{\gamma_{ml}}{FO_{ml}} + \sum_{k=1}^{2} \frac{\psi_{mk}}{LS_{mk}} \right) + \sum_{p=1}^{3} \frac{\xi_p}{S_p} + \sum_{r=1}^{4} \frac{\beta_r}{U_r} \right] \zeta_3 (\theta_3 - a_5) \\
&\quad + \left(\frac{\xi_2 F}{S_2^2} - \frac{\xi_1 F}{S_1^2} \right) \left(\frac{|\theta_3|}{\theta_3} \right), \\
h_1 &= 1 + \frac{\beta_1 F}{U_1^2}, \qquad h_2 = 1 + \frac{\beta_2 F}{U_2^2}, \qquad h_3 = 1 + \frac{\beta_3 F}{U_3^2}, \qquad h_4 = 1 + \frac{\beta_4 F}{U_4^2}.
\end{aligned}
$$

Now, if we are given parameters $\delta_j > 0$ for $j = 1, \ldots, 4$, called *convergence parameters*,

then we can define the translational and rotational velocities as

$$\begin{aligned}
-\delta_1 v &= (f_1+f_3+f_5+f_7)\cos\theta_1+(f_2+f_4+f_6+f_8)\sin\theta_1+h_1u_1,\\
-\delta_2\omega_1 &= -\left(f_1+\frac{1}{2}f_3+f_5+f_7\right)\ell_0\sin\theta_1+\left(f_2+\frac{1}{2}f_4+f_6+f_8\right)\ell_0\cos\theta_1\\
&\quad-\left(f_1+\frac{1}{2}f_5+f_7\right)\ell_1\sin\theta_Q+\left(f_2+\frac{1}{2}f_6+f_8\right)\ell_1\cos\theta_Q\\
&\quad-\left(f_1+\frac{1}{2}f_7\right)\ell_2\sin\theta_T+\left(f_2+\frac{1}{2}f_8\right)\ell_2\cos\theta_T+g_1+h_2u_2,\\
-\delta_3\omega_2 &= -\left(f_1+\frac{1}{2}f_5+f_7\right)\ell_1\sin\theta_Q+\left(f_2+\frac{1}{2}f_6+f_8\right)\ell_1\cos\theta_Q\\
&\quad-\left(f_1+\frac{1}{2}f_7\right)\ell_2\sin\theta_T+\left(f_2+\frac{1}{2}f_8\right)\ell_2\cos\theta_T+g_2+h_3u_3,\\
-\delta_4\omega_3 &= -\left(f_1+\frac{1}{2}f_7\right)\ell_2\sin\theta_T+\left(f_2+\frac{1}{2}f_8\right)\ell_2\cos\theta_T+g_3+h_4u_4.
\end{aligned}$$

Hence, along a trajectory of system (1) in $D(L)$, we have

$$\dot{L}_{(1)}(\mathbf{x}) = -\delta_1 v^2-\delta_2\omega_1^2-\delta_3\omega_2^2-\delta_4\omega_3^2\le 0,$$

provided our feedback nonlinear controllers are of the form

$$\left.\begin{aligned}
u_1 &= -\left[\delta_1 v+(f_1+f_3+f_5+f_7)\cos\theta_1+(f_2+f_4+f_6+f_8)\sin\theta_1\right]/h_1,\\
u_2 &= -\left[\delta_2\omega_1-\left(f_1+\frac{1}{2}f_3+f_5+f_7\right)\ell_0\sin\theta_1+\left(f_2+\frac{1}{2}f_4+f_6+f_8\right)\ell_0\cos\theta_1\right.\\
&\quad-\left(f_1+\frac{1}{2}f_5+f_7\right)\ell_1\sin\theta_Q+\left(f_2+\frac{1}{2}f_6+f_8\right)\ell_1\cos\theta_Q\\
&\quad\left.-\left(f_1+\frac{1}{2}f_7\right)\ell_2\sin\theta_T+\left(f_2+\frac{1}{2}f_8\right)\ell_2\cos\theta_T+g_1\right]/h_2,\\
u_3 &= -\left[\delta_3\omega_2-\left(f_1+\frac{1}{2}f_5+f_7\right)\ell_1\sin\theta_Q+\left(f_2+\frac{1}{2}f_6+f_8\right)\ell_1\cos\theta_Q\right.\\
&\quad\left.-\left(f_1+\frac{1}{2}f_7\right)\ell_2\sin\theta_T+\left(f_2+\frac{1}{2}f_8\right)\ell_2\cos\theta_T+g_2\right]/h_3,\\
u_4 &= -\left[\delta_4\omega_3-\left(f_1+\frac{1}{2}f_7\right)\ell_2\sin\theta_T+\left(f_2+\frac{1}{2}f_8\right)\ell_2\cos\theta_T+g_3\right]/h_4.
\end{aligned}\right\}\qquad(8)$$

We note that the controllers u_1, u_2, u_3 and u_4 are continuous on $D(L)$, and that $\mathbf{x}_e = (a_1, a_2, a_3, a_4, a_5, 0, 0, 0, 0)$ is an equilibrium point of system (1) given the above choices of the controllers.

The following theorem ends our discussions thus far:

Theorem 1 *The equilibrium point* $\mathbf{x}_e$ *of system* (1) *is stable provided the controllers,* u_1*,* u_2*,* u_3*, and* u_4*, are as defined in* (8)*.*

In this paper, we attempt to show that we can have, at least, a Lyapunov stable system with continuous feedback laws for navigation, steering, and point and posture stabilities. Then, because of the inherent property of the Lyapunov stability, there could be initial conditions that give asymptotic stability. For now, we are satisfied with searching for these initial conditions numerically via the computer. This is, admittedly, still a long way from proving asymptotic stability, but we have now a starting point for using continuous control laws that guarantee, for some initial conditions, point and posture stabilities. Indeed, extensive simulations using the proposed control laws hint to the existence of initial conditions guaranteeing asymptotic stability. A challenging future problem is to attempt to identify, possibly via the LaSalle Invariant Principle, a set of these initial conditions. This problem may not be unsolvable given that the approach of proving Lyapunov stability and then using the control laws to make the system asymptotically stable via a Lasalle invariance principle argument, has been shown to be effective in stabilizing related nonlinear control systems such as the Lagrangian and Hamiltonian systems. This is the direction taken in the recent works of Bloch et al. ([1], [2]) and Chang et al. [4]. Indeed, using LaSalle's method, it is now possible to ensure asymptotically stability in point-mass based obstacle avoidance systems, as shown in the work of Ha and Shim in 2001 [8].

4.2 Parameters

An indispensable feature of our Lyapunov function is its control and convergence parameters. The *control parameters*, α_s, ξ_p, β_r, γ_{ml} and ψ_{mk}, increase the freedom of maneuverability of the mobile manipulator to better account for the fixed obstacles, which include the limitations on velocity and the steering angle of the platform as well. For example, increasing the value of γ_{3l} will make link 2 avoid the fixed circular obstacle from a greater distance. The *convergence parameters*, δ_j, for $j = 1, \ldots, 4$, affect the rate of convergence of the manipulator to its desired configuration. The authors have also used the *safety parameters* and the *angle-gain parameters* efficiently to get the desired outcomes.

5 Simulations

In this section, we demonstrate the simulation results for our mobile manipulator navigating in a constrained workspace cluttered with fixed obstacles. We verify numerically the stability results obtained from the Lyapunov function.

5.1 Scenario 1

In this example, we consider a simple setup where the mobile manipulator maneuvers from an initial to a final configuration, whilst avoiding a fixed obstacle in its path, with no attempt made to fix its final orientation. Assuming the use of appropriate units, the corresponding initial conditions, workspace boundary restrictions and velocity constraints are listed below:

1. **Robot parameters:** $\ell_0 = 2$, $b_0 = 1$ and $\ell_1 = \ell_2 = 1.2$.
2. **Initial configuration:**
   Rectangular Position: $(x(0), y(0)) = (5, 5)$.
   Angular Positions: $\theta_1(0) = \pi/4$, $\theta_2(0) = \pi/3$ and $\theta_3(0) = -2\pi/3$.
   Velocities: $v(0) = 5$; $\omega_1(0) = \omega_2(0) = \omega_3(0) = \pi/360$.
3. **Target:** Center: $(a_1, a_2) = (25, 25)$, Radius: $r_T = 0.5$.
4. **Fixed obstacle:** Center: $(p_{11}, p_{12}) = (15, 15)$, Radius: $rad_1 = 3$.
5. **Physical Limitations:** Maximum translational velocity: $v_{\max} = 10$. Maximum steering angle $\phi_{\max} = 70^o$. The maximum rotational velocities of link 1 and link 2 are fixed at $\omega_{1\max} = \omega_{2\max} = 1$.
6. **Clearance and safety parameters:** $\epsilon_1 = \epsilon_2 = 0.1$, $\epsilon_3 = 0.3$.
7. **Control parameters:** $\alpha_s = 0.01$ for $s = 1, 2, \ldots, 8$; $\xi_p = 0.1$ for $p = 1, 2, 3$; $\beta_r = 1$ for $r = 1, \ldots, 4$; $\gamma_{m1} = 0.5$, for $m = 1, 2, 3$; $\psi_{mk} = 0$, for $m = 1, 2, 3$ and $k = 1, 2$.
8. **Angle-gain parameters:** $\zeta_1 = \zeta_2 = \zeta_3 = 0$.
9. **Convergence parameters:** $\delta_j = 50$, for $j = 1, \ldots, 4$.
10. **Workspace Boundaries:** $\eta_1 = \eta_2 = 28$.

The nonlinear controllers u_1, u_2, u_3 and u_4 were simulated to generate a feasible robot trajectory as seen in Figure 2. With the initial conditions described above, the control laws ensured a nice convergence of the system state to the equilibrium state, whilst satisfying all the underlying constraints. For the numerical integration of system (1), a fourth order Runge-Kutta method was utilized.

Figure 3 shows the Lyapunov function and its time derivative along the system trajectory. Not only does the figure show that the conditions of Theorem 1 have been satisfied but it also gives us the information where the mobile manipulator has accelerated or decelerated. An increase in $\dot{L}(\mathbf{x})$ indicates that the manipulator is decelerating, where as a decrease in $\dot{L}(\mathbf{x})$ indicates that the manipulator is accelerating. Figure 4 to 7 show explicitly the

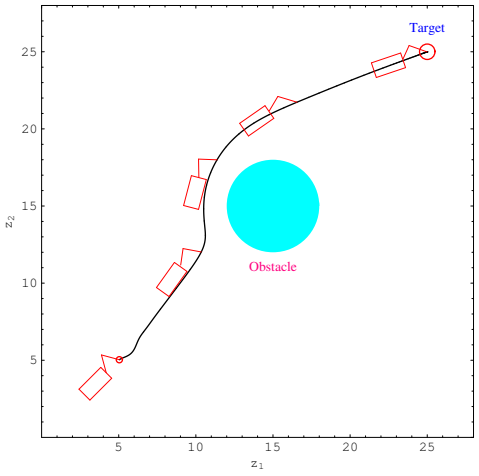

Fig. 2: Scenario 1. Trajectory of the 2-link mobile manipulator in a constrained workspace.

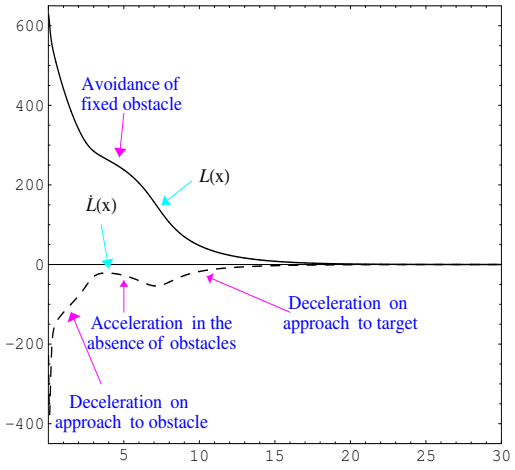

Fig. 3: Scenario 1. Behavior of the Lyapunov function $L(\mathbf{x})$ and its time derivative $\dot{L}(\mathbf{x})$

time evolution of the relevant state-space variables along the trajectory of the mobile manipulator. One can clearly notice the asymptotic convergence of the accelerations at the final configuration implying the effectiveness of the new controllers.

5.2 Scenario 2

In this second example, not only do we require that the mobile manipulator stays within the workspace and avoids multiple fixed obstacles, but also we require it to be parked correctly inside a row-structured parking bay. We have used the same parameters as those in Scenario 1, and those that differ are listed below. The desired final configuration is also listed.

1. **Initial configuration:**
   Rectangular Position: $(x(0), y(0)) = (5, 5)$.
   Angular Positions: $\theta_1 = \pi/4$, $\theta_2 = \pi/3$ and $\theta_3 = -2\pi/3$.
   Velocities: $v = 4$;$\omega_1 = \omega_2 = \omega_3 = \pi/360$.

2. **Target:** Center: $(a_1, a_2) = (27, 23)$.

3. **Desired Final Orientations:** $(a_3, a_4, a_5) = (0^o, 45^o, -90^o)$.

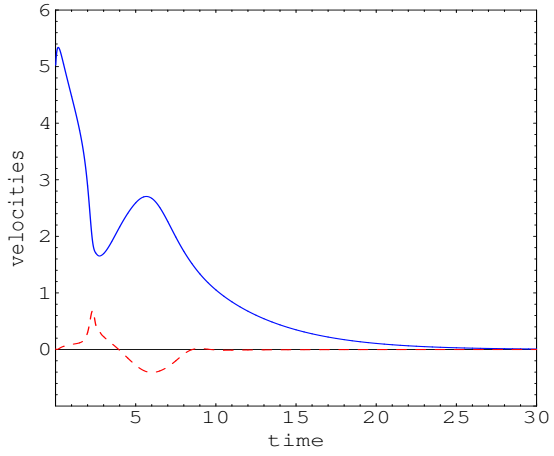

Fig. 4: Scenario 1. The translational v (solid line) and rotational ω_1 velocities of the platform. They satisfy the constraints (5) and (6), respectively.

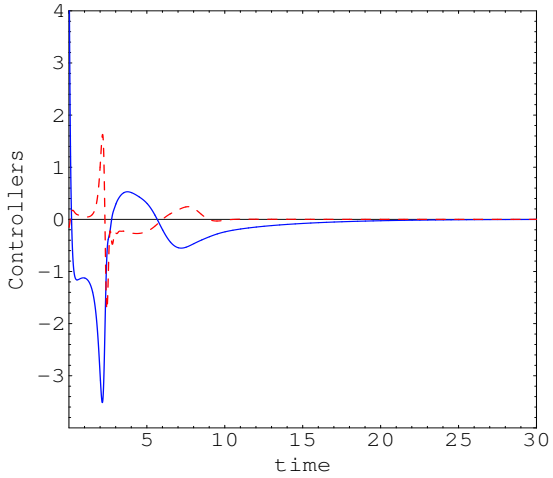

Fig. 5: Scenario 1. The translational u_1 (solid line) and rotational u_2 accelerations of the platform.

4. **Fixed obstacles:**
   FO1: Centered at $(p_{11}, p_{12}) = (9, 9)$ with radius $rad_1 = 1.5$.
   FO2: Centered at $(p_{21}, p_{22}) = (10, 18)$ with radius $rad_2 = 1.5$.
   FO3: Centered at $(p_{31}, p_{32}) = (18, 16)$ with radius $rad_3 = 2$.

5. **Control parameters:** $\alpha_s = 0.01$, for $s = 1, 2, \ldots, 8$; $\xi_p = 0.1$, for $p = 1, 2, 3$;
   $\beta_r = 1$ for $r = 1, \ldots, 4$; $\gamma_{m1} = \gamma_{m2} = \gamma_{m3} = 1$, for $m = 1, 2, 3$;
   $\psi_{mk} = 2.5$ for $m = 1, 2, 3$ and $k = 1, 2$.

6. **Angle-gain parameters:** $\zeta_1 = \zeta_2 = \zeta_3 = 1$.

7. **Convergence parameters:** $\delta_j = 50$, for $j = 1, \ldots, 4$.

8. **Parking bay parameters:** Can be obtained from Fig. 8

Figure 8 shows a feasible trajectory from the initial to the final states. In the final phase, the platform and the links achieved a pre-determined final orientation. Under the initial conditions, limitations and restrictions, the control laws ensured convergence of the system state to the equilibrium state.

To illustrate the convergent property of the navigation laws, we have generated the graphs of velocity and acceleration components (as shown in Figures 9 to 12). The evolution of the Lyapunov function is similar to Figure 3.

The efficiency of the control laws were tested with various other initial configurations. Convergence was observed for all cases, provided the initial configurations did not intersect

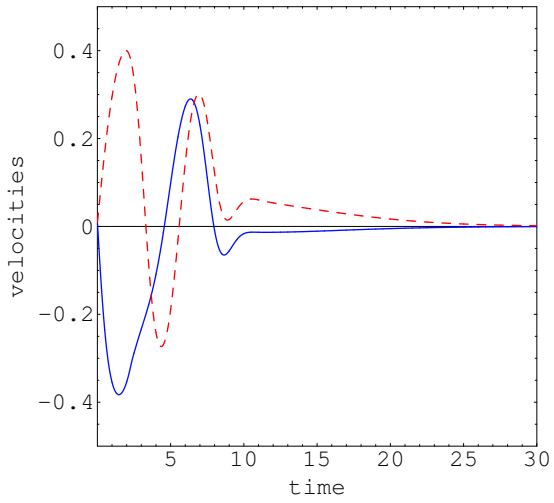

Fig. 6: Scenario 1. The rotational velocities ω_2 of link 1 (solid line) and ω_3 of link 2.

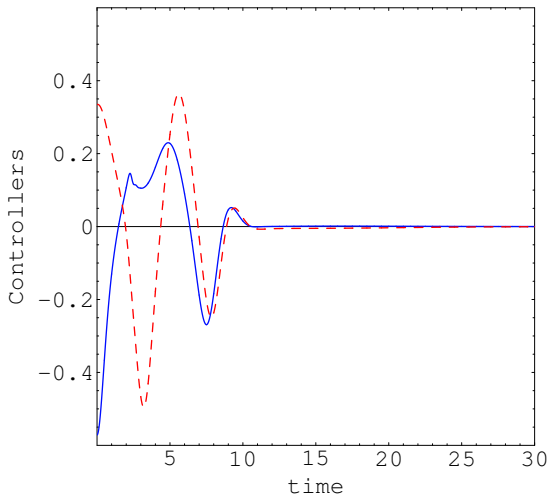

Fig. 7: Scenario 1. The rotational accelerations u_3 of link 1 (solid line) and u_4 of link 2.

with the obstacle space. Mobile manipulators (with any initial orientation) placed near the outskirts of the parking bay did converge to the desired position. In each case, there was a nice convergence to the target with θ_1, θ_2 and θ_3 in a small neighborhood of the desired orientations. Better trajectories were achievable via fine tunings of the control and convergence parameters, the values of which were quite different for each set of initial conditions.

6 Conclusion

We have presented a set of continuous time-invariant acceleration control laws that successfully tackle the multi-tasking problem posed in this paper. Synthesis of these controllers for our dynamic system was for the first time attempted via the Lyapunov-based approach, which guaranteed stability of the system. The new motion planning algorithm enabled us to obtain collision-free trajectories from initial to desired states within a constrained environment cluttered with fixed obstacles, whilst satisfying the holonomic, nonholonomic, kinematic and dynamic constraints associated with the system. Although computationally intensive, the Lyapunov-based approach can invariably be extended to three-dimensional cases as well.

Future work includes (a) searching for a similar Lyapunov-based algorithm that guarantees asymptotic posture stability of mobile manipulators, (b) modifying the proposed control

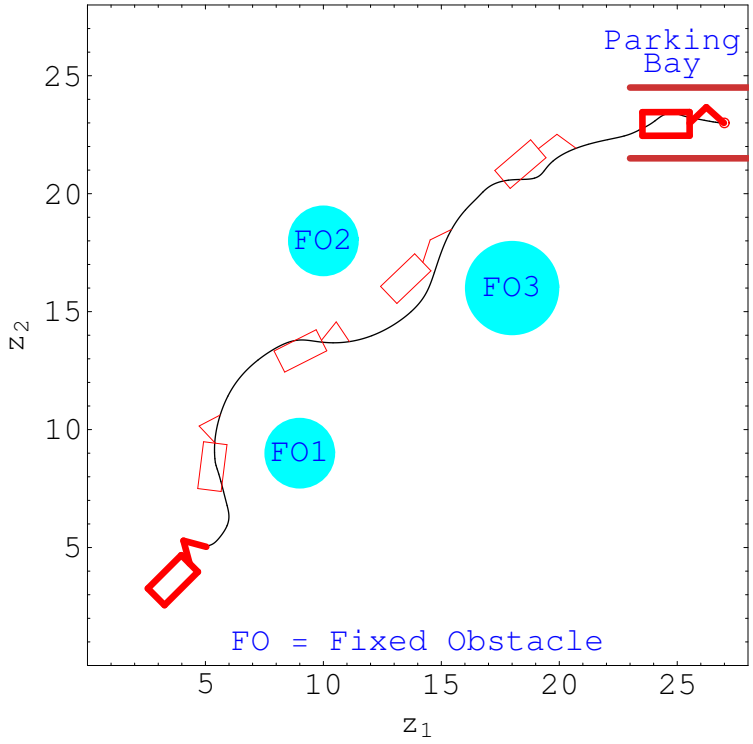

Fig. 8: Scenario 2. Trajectory of the mobile manipulator in a constrained workspace.

algorithm for motion planning in dynamic environments, which include mobile and moving obstacles, (c) generalizing the algorithm for a multiple-task that includes motion planning, collision avoidance, and parking maneuverability of mobile manipulators with a spatial manipulator, and (d) theoretically proving the existence of an invariant set of initial conditions that guarantee stabilization of our kinodynamical system.

7 Acknowledgment

The authors would like to express their sincere thanks to the referees whose comments have resulted in this improved version of the paper.

References

[1] A.M. Bloch, P. Crouch, J. Baillieul, and J. Marsden. *Nonholonomic Mechanics and Control*. Springer-Verlag, New York, 2003.

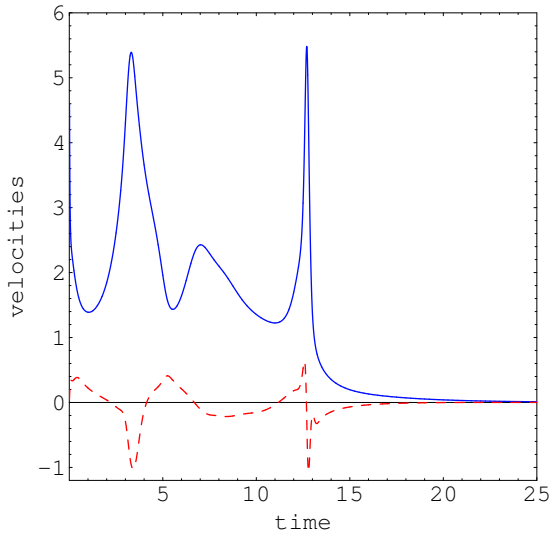

Fig. 9: Scenario 2. The translational v (solid line) and rotational ω_1 velocities of the platform. They satisfy the constraints (5) and (6), respectively.

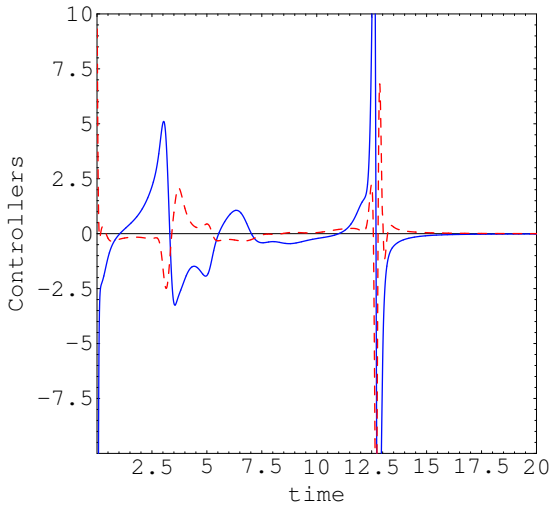

Fig. 10: Scenario 2. The translational u_1 (solid line) and rotational u_2 accelerations of the platform.

[2] A.M. Bloch, N. E. Leonard, and J. E. Marsden. "Matching and Stabilization by the Method of Controlled Lagrangians". In *Proc. of the 37th IEEE Conference on Decision and Control*, pages 1446–1451, Tampa(FL), USA, December 1998.

[3] C. I. Connolly, J. B. Burns, and R. Weiss. "Path Planning using Laplace's Equation". In *Proc. 1990 IEEE International Conference on Robotics and Automation*, pages 2102–2106.

[4] D. D. Chang, A. M. Bloch, N. Leonard, J. E. Marsden, and C. Woolsey. "The Equivalence of Controlled Lagrangian and Controlled Hamilton Systems". *ESAIM: Control, Optimization, and the Calculus of Variations - Special Issue Dedicated to J. L. Lions*, 8:393–422, 2002.

[5] G. Foulon, J.-Y. Fourquet, and M. Renaud. *Experimental Robotics V: Lecture Notes in Control and Information Systems*, chapter Control of a Rover-mounted Manipulator, pages 140–151. Springer, 1998.

[6] G. Foulon, J.-Y. Fourquet, and M. Renaud. "Planning Point to Point Paths for Non-holonomic Mobile Manipulators". In *IEEE/RSJ International Conference on Intelligent Robots and Systems*, pages 374–379, Victoria, Canada, October 1998.

[7] G. Foulon, J.-Y. Fourquet, and M. Renaud. "Coordinating Mobility and Manipulation Using Non-holonomic Mobile Manipulators". *Control Engineering Practice*, 7:391–399, 1999.

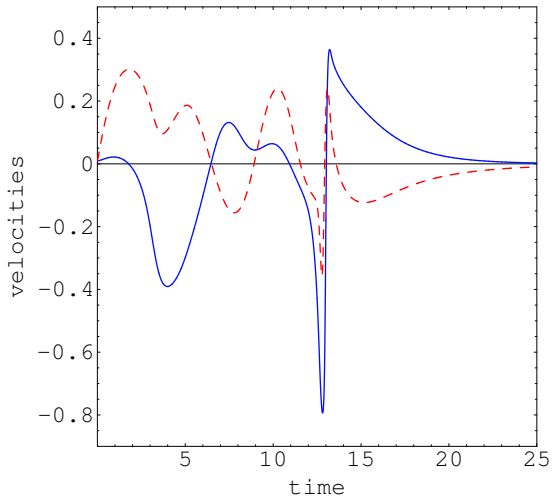

Fig. 11: Scenario 2. The rotational velocities ω_2 of link 1 (solid line) and ω_3 of link 2.

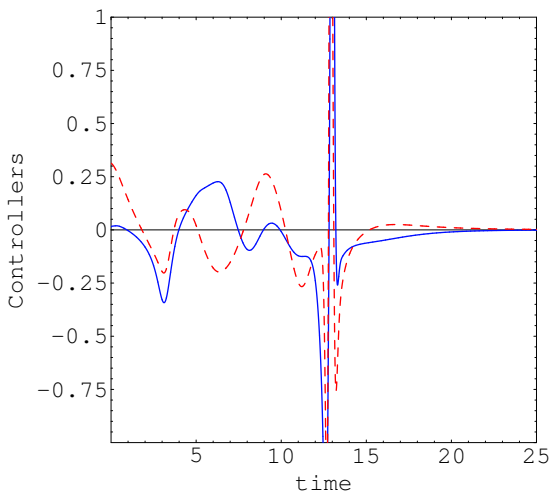

Fig. 12: Scenario 2. The rotational accelerations u_3 of link 1 (solid line) and u_4 of link 2.

[8] J. Ha and J. Shim. "An Asymptotic Stability involving Collision and Avoidance". *Korean Journal of Computational and Applied Mathematics*, 8:605–616, 2001.

[9] Q. Huang, S. Sugano, and K. Tanie. "Motion Planning for a Mobile Manipulator Considering Stability and Task Constraints". In *Proceedings of the IEEE International Conference on Robotics and Automation*, pages 2192–2198, Leuven, Belgium, May 1998.

[10] O. Khatib. "Real Time Obstacle Avoidance for Manipulators and Mobile Robots". *International Journal of Robotics Research*, 7(1):90–98, 1986.

[11] J. Kim and P. Khosla. "Real-time Obstacle Avoidance using Harmonic Potential Fuunctions". pages 790–796.

[12] A. Matsikis, F. Schulte, F. Broicher, and K. F. Fraiss. "A Behaviour Coordination Manager for a Mobile Manipulator". In *Proceedings of the IEEE/RSJ Int. Conf. on Intelligent Robots and Systems*, pages 174–181, Las Vegas, USA, 2003.

[13] E. Papadopoulos, I. Papadimitriou, and I. Poulakakis. "Polynomial-based Obstacle Avoidance Techniques for Nonholonomic Mobile Manipulator Systems". *Robotics and Autonomous Systems*, 41(4):229–247, 2005.

[14] E. Papadopoulos, I. Poulakakis, and I. Papadimitriou. "On Path Planning and Obstacle Avoidance for Nonholonomic Mobile Manipulators: a Polynomial Approach". *International Journal of Robotics Research*, 21(4):367–383, 2002.

[15] E. Papadopoulos and J. Poulakakis. "Planning and Model-based Control for Mobile Manipulators". In *Procs of the IROS Conference on Intelligent Robots and Systems*, Takamatsu, Japan, 2000.

[16] G. J. Pappas and K. J. Kyriakopoulos. "Stabilization of Non-holonomic Vehicle Under Kinematic Constraints". *International Journal of Control*, 61(4):933–947, 1995.

[17] C. Perrier, P. Dauchez, and F. Pierrot. "A Global Approach for Motion Generation of Non-holonomic Mobile Manipulator". In *Proceedings of the IEEE International Conference on Robotics and Automation*, pages 2971–2976, Leuven, Belgium, May 1998.

[18] E. Rimon. "Exact Robot Navigation Using Artificial Potential Functions". *IEEE Transactions on Robotics and Automation*, 8(5):501–517, 1992.

[19] H. Seraji. "A Unified Approach to Motion Control of Mobile Manipulators". *International Journal of Robotics Research*, 17(2):107–118, 1998.

[20] B. Sharma and J. Vanualailai. "Lyapunov Stability of a Nonholonomic Car-like Robotic System". *Nonlinear Studies*, 14(2):143–160, 2007.

[21] B. Sharma, J. Vanualailai, and A. Chandra. "Dynamic Trajectory Planning of a *standard* Trailer System". *Far East Journal of Applied Mathematics*, 28(3):465–486, 2007.

[22] B. Sharma, J. Vanualailai, and S. Nakagiri. "Posture Control and Stability of a *general* 1-Trailer System: a Lyapunov Approach". In *RIMS Symposium*, pages 134–143, Kyoto University, Japan, November 2006.

[23] T.G. Sugar and V. Kumar. "Control of Cooperating Mobile Manipulators". *IEEE Transactions on Robotics and Automation*, 18(1):94–103, 2002.

[24] H. G. Tanner, S. Loizou, and K. J. Kyriakopoulos. "Nonholonomic Navigation and Control of Cooperating Mobile Manipulators". *IEEE Transactions on Robotics and Automation*, 19(3):53–64, 2003.

[25] L. Tarassenko and A. Blake. "Analogue Computation of Collision-free Paths". In *Procs. 1991 IEEE International Conference on Robotics and Automation*, pages 540–545.

[26] J. Vanualailai, S. Nakagiri, and J. Ha. "A Solution to Two-dimension Findpath Problem". *Dynamics and Stability of Systems*, 13:373–401, 1998.

[27] J. Vanualailai and B. Sharma. "Moving a Robot Arm: an Interesting Application of the Direct Method of Lyapunov". *CUBO: A Mathematical Journal*, 6(3):131–144, 2004.

[28] D. Xu, H. Hu, C. A. A. Calderon, and M. Tan. "Motion Planning for a Mobile Manipulator with Redundant DOFs". *International Journal of Information Technology*, 11(11):1–10, 2005.

[29] Y. Yamamoto and X. Yun. "Coordinated Obstacle Avoidance of a Mobile Manipulator". In *Proc. IEEE International Conference on Robotics and Automation*, volume 3, pages 2255–2260, May 1995.

Bibhya N. Sharma received his Master's degree in mathematics from the University of the South Pacific, Fiji, in 1998. He is completing his PhD degree in applied mathematics from the same university. He is currently a lecturer in Mathematics with the School of Computing, Information and Mathematical Sciences of the Faculty of Science and technology, University of the South Pacific. He is also the Coordinator of the Mathematics Division. His main fields of interest are dynamics of nonlinear systems, robotics and artificial neural networks.

Jito Vanualailai obtained his PhD from Kobe University, Japan, in 1994, in the area of the stability analysis of nonlinear systems. He joined the University of the South Pacific, Fiji, thereafter, as a lecturer in mathematics. He has remained at the same university since then, and is now an Associate Professor of Mathematics and is the Head of the School of Computing, Information and Mathematical Sciences. Dr. Jito Vanualailai publishes in the areas of Volterra integro-differential equations, artificial neural networks and robotics.

Avinesh Prasad received his Bachelor's degree in Mathematics and Physics and completed his Master's degree in applied mathematics in 2008 at the University of the South Pacific, Fiji Islands. Since 2006, he has been with the School of Computing, Information and Mathematical Sciences, University of the South Pacific, Fiji Islands. His area of interest are dynamics of nonlinear systems and robotics.